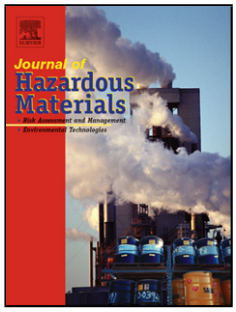

Title: Multilayer Films of Layered Double Hydroxide/Polyaniline and Their Ammonia Sensing Behavior

Author: Dong-Mei Xu Mei-Yu Guan Qing-Hong Xu Ying Guo

PII: S0304-3894(13)00600-6
DOI: http://dx.doi.org/doi:10.1016/j.jhazmat.2013.08.034
Reference: HAZMAT 15336

To appear in: *Journal of Hazardous Materials*

Received date: 22-1-2013
Revised date: 11-7-2013
Accepted date: 13-8-2013

Please cite this article as: D.-M. Xu, M.-Y. Guan, Q.-H. Xu, Y.G. *<ce:inter-ref id="intr0005" xlink:href="mailto:guoying@mail.buct.edu.cn">guoying@mail.buct.edu.cn</ce:inter-ref><ce:inter-ref id="intr0010" xlink:href="mailto:guoyingbuct@gmail.com">guoyingbuct@gmail.com</ce:inter-ref> Multilayer Films of Layered Double Hydroxide/Polyaniline and Their Ammonia Sensing Behavior, *Journal of Hazardous Materials* (2013), http://dx.doi.org/10.1016/j.jhazmat.2013.08.034

Multilayer Films of Layered Double Hydroxide/Polyaniline and Their Ammonia Sensing Behavior

Dong-Mei Xu, Mei-Yu Guan, Qing-Hong Xu, Ying Guo*

State Key Laboratory of Chemical Resource Engineering, Beijing University of Chemical Technology, P.O. Box 98, Beijing, 100029, P.R. China

*To whom correspondence should be addressed, Tel: (+86)-10-64412115.

Email: guoying@mail.buct.edu.cn, guoyingbuct@gmail.com

Abstract: This paper reports the fabrication of layered double hydroxide (LDH)/conductive polymer multilayer films by alternate assembly of exfoliated ZnAl-LDH nanosheets and polyaniline (PANI) on silicon wafer substrates using the layer-by-layer (LBL) deposition technology. UV-vis absorption spectroscopy indicates a stepwise and regular growth of the $(LDH/PANI)_n$ multilayer films upon increasing deposition cycles. Scanning electron microscopy (SEM) and atomic force microscopy (AFM) demonstrate that the surfaces of the films are microscopy smooth and uniform with a thickness of 2 nm per bilayer. Furthermore, the resulting $(LDH/PANI)_n$ multilayer films possess high selectively response to ammonia at room temperature. The presence of LDH nanosheets plays a critical role on the gas sensing for the pure PANI film has very low response to ammonia. The LBL assembly process based on LDH combines the conducting polymer and nano-inorganic material, which provides opportunities to develop new inorganic-organic films for gas sensing.

Keywords: layered double hydroxide; polyaniline; layer-by-layer; ammonia sensing.

1. Introduction:

It is well known that ammonia has been widely applied in food technology, chemical engineering, firepower plant, medical diagnosis, and refrigeration industrial processes etc.[1-3]. However, ammonia is also a poisonous gas, which could bring a threat to the human health. For instance, even short-term exposure to 1000 ppm or above ammonia would lead to a fatal respiratory system and lung disorder [4-6]. Accordingly, a leak in the systems, including the chemical industry, fertilizer factories and refrigeration systems where make use of almost pure ammonia, would definitely result in a serious life-threatening situation [1]. For that reason, there is an increasing demand to fabricate ammonia gas sensors with good stability, considerable sensitivity as well as high selectivity. Nowadays, the most common ammonia gas sensors available on the market are semiconductor oxides sensors, but always with a high operation temperature. Compared with the semiconductor oxides, the advantages of conducting polymers are their diversity, easy synthesis and their gas responses particularly at room temperature [7, 8]. Among the conducting polymers, polyaniline (PANI) has recently achieved widespread attentions for its high yield, good environmental stability, appreciable conductivity and interesting redox behavior controlled by simply doping/dedoping approach [9-12]. However, similar to other polymers, pure PANI used as gas sensor is limited in application due to its poor processing performance [13]. For solving this problem, many kinds of hybrid films based on PANI have been prepared and fabricated for gas detection. Particularly, these hybrid films with PANI and inorganic materials have shown the extended application of PANI as well as its

improved gas sensing behavior [14-16], which is partly attributed to its better process ability and enhanced heat resistance result from the addition of inorganic components [17].

Nevertheless, the fabrication and manufacture techniques are as important as the preparation of new materials themselves. Nowadays, a large number of gas sensing materials have been prepared as thin film which involves namely the physical or chemical techniques. The physical techniques include chemical vapor deposition, thermal vapor deposition, sputtering, laser ablation etc, whereas the sol-gel, Langmuir-Blodgett, spin coating, Layer by layer (LBL) assembly etc. are belong to chemical routes [18]. The advantage of gas sensing films achieved *via* chemical route is that large quantity of processable nanostructures can be obtained at a cost-effective, highly-scalable and mild reaction condition. In particular, for organic-inorganic hybrid thin films, since the vapor pressure and decomposition temperature of the organic and inorganic individual compounds differ significantly, they can not be prepared by the standard physical techniques [19]. As such, among the chemical methods that have been developed for preparing films, LBL assembly, based on sequential adsorptions of oppositely charged species in solution, is an advisable method for the deposition of organic-inorganic hybrid thin films owing to the merits of LBL assembly, such as low cost, room temperature process, high reproducibility, and especially the controllable thickness at a molecular scale [20, 21].

Layered double hydroxide (LDH) is a class of anionic layered clay with a general formula of $[M^{2+}_{1-x}M^{3+}_{x}(OH)](A^{n-})_{x/n}\cdot yH_2O$, in which M^{2+} and M^{3+} are divalent and trivalent

metal cations respectively, and A^{n-} is the intercalated guest anion [22]. LDH can be used as a host matrix for the orientation and dispersion of interlayer anions, in order to afford tailored catalytic [23], sensor [24], optical [25], thermal [26] and magnetic [27] functional materials, etc. Admitting that there are reports about electrochemistry films of LDH-supported polyaniline, those films have been applied in solution phase and couldn't be obtained with controlled morphology and structure [28]. It is worth noting that LDH can be exfoliated into positively charged nanosheets, which can be used to construct inorganic-organic multilayer films by layer-by-layer (LBL) assembly technique which involves the alternative deposition of LDH nanosheets and polymers by the driving force between them, such as electrostatic force, hydrogen bonding, covalent bonding, coordination bonding, etc. [29]. Moreover, to the best of our knowledge, there still lacks reports on gas sensing properties of LDH nanosheets and conductive polymer films obtained by LBL process till now. Therefore, in this paper ZnAl-LDH/PANI multilayer and ultrathin films have been fabricated with uniform morphology, ordered structure and controllable thickness by LBL assembly of PANI with exfoliated ZnAl-LDH nanosheets (Scheme 1) and their resistance change in different gas phase has been further observed. It turns out that the ZnAl-LDH/PANI multilayer films show higher ammonia response compared with the PANI film alone. Therefore, it can be concluded that the ZnAl-LDH nanosheets have provided a confined and stable microenvironment for the immobilization of PANI as well as increasing the reaction spaces between PANI and gas molecules. This assembly under the nanometer

scale has resulted in a high dispersion of PANI with uniform orientation and avoidable aggregation, which brought out the high ammonia response of PANI.

2. Experimental Section

2.1 Preparation of ZnAl-LDH Nanosheets

The starting materials were $Zn(NO_3)_2 \cdot 6H_2O$ (99.0% purity from Xilong Chemical Co., Ltd), $Al(NO_3)_3 \cdot 9H_2O$ (99.0% purity from Xilong Chemical Co., Ltd), urea (99.0% purity from Xilong Chemical Co., Ltd), methanol (AR from Beijing Chemical Works) and HNO_3 (AR from Beijing Chemical Works).

In this paper, CO_3^{2-} intercalated ZnAl-LDH (ZnAl-CO_3^{2-}-LDH) with a high degree of crystallization was synthesized using a similar procedure reported by Sasaki [30]: $Zn(NO_3)_2 \cdot 6H_2O$ (10 mM), $Al(NO_3)_3 \cdot 9H_2O$ (5 mM) and urea (35 mM) were dissolved and mixed in aqueous solution and the solution had been further heated at 97^oC under refluxing and continuous magnetic stirred for 2 days. The obtained product ZnAl-CO_3^{2-}-LDH was washed with water and ethanol for several times before being dried in air at 60^oC.

As NO_3^- interacted LDH is found to possess excellent delamination behavior, the sample of ZnAl-CO_3^{2-}-LDH was converted to NO_3^- intercalated (ZnAl-NO_3^--LDH) by ion exchange process using 6.6 mM HNO_3 with 90 mL methanol solution [31] while being purged by nitrogen gas for 3-5 hours at ambient temperature. The resulting precipitate was separated through centrifugation before being washed with methanol and dried under vacuum.

At last, 0.5 g of ZnAl NO_3^--LDH was shaken in a 500 mL formamide solution for

72 h to produce a colloidal suspension of exfoliated ZnAl-LDH nanosheets. To remove the unexfoliated particles, the resulting translucent colloidal suspension was further treated by centrifugation at 6000 rmp for 4 min. After that, the rest of colloidal suspension was transparent and stable, in which a clear Tyndall light was observed.

2.2 Fabricate of (ZnAl-LDH/PANI)$_n$ Multilayer films

The (ZnAl-LDH/PANI)$_n$ multilayer films were fabricated through the LBL assembly technique. The quartz glass and silicon substrate were immerse and cleaned beforehand in concentrated methanol/HCl (V/V = 1/1) and concentrated H_2SO_4 for 20 min each, and then in a piranha solution 98% H_2SO_4/30% H_2O_2 (7:3) for 30 min. After every procedure, the quartz substrate was rinsed and washed thoroughly with deionized water and dried before next immerse. During the assembly process, the cleaned substrate was firstly dipped into the colloidal suspension of ZnAl-LDH nanosheets for 10 min followed by being washed thoroughly with deionized water. Afterwards, the substrate was dried before being treated with 0.5 g/L PANI (emeraldine salt, average Mw > 15,000 from SIGMA-ALORICH) in a solvent of 1-Methyl-2-pyrrolidone (99.0% purity from J&KCHEMICA) for 10 min. The deposition procedures for ZnAl-LDH nanosheets colloidal and PANI solution were cycled and repeated for n times to obtain (ZnAl-LDH/PANI)$_n$ multilayer films (Scheme 1). The resulting films were dried under nitrogen gas flow for 2 min at ambient temperature.

2.3 Characterization

X-ray diffraction (XRD) characterizations were conducted on a Rigaku XRD-6000 diffractometer using Cu Kα radiation (λ = 0.15418 nm) at an accelerating voltage of

40 kV and current of 30 mA. The solid UV-vis spectra of mutilayer films on quartz glass were recorded in a Shimadzu U-3000 spectrophotometer. The morphology and thickness of mutilayer films on silicon wafer were investigated using a scanning electron microscope (SEM Hitachi S-4700) with the accelerating voltage of 20 kV. The surface roughness of mutilayer films on silicon wafer was studied using an Agilent atomic force microscopy (AFM-5500).

2.4 Gas Sensing Measurements

The gas sensing measurement of the $(ZnAl\text{-}LDH/PANI)_n$ multilayer films were conducted on a CGS-1TP intelligent gas sensing analysis system (Beijing Elite Tech. Co. Ltd. China). This multifunctional system, which has been described before [24], consists of heating system, gas distribution system, probe adjustment system, vacuum system, and data acquisition system. The heating system offers an external temperature control from room temperature to about 500^{o}C with a precision of 1^{o}C, which could adjust the sensor temperature directly. The gas response is designated as R_g/R_a, where R_a is the sensor resistance in air (base resistance) and R_g is that in the target gas. The time taken by the sensor resistance to change from R_a to $R_a + 90\% \times (R_g - R_a)$ is defined as response time after the target gas being introduced to the sensor, and the time taken from R_g to $R_g - 90\% \times (R_g - R_a)$ is defined as recovery time after the ambience being replaced by air.

The gas sensitive characteristics of multilayer films on silicon wafer were investigated by recording their resistances after being alternately exposed to different concentration of gases at certain temperature. All the multilayer films were pretreated at

100°C for 2 h, and were cooled to room temperature (25°C) for gas sensing measurement. For comparison, the pure PANI film for gas sensing measurement was obtained by dropping with PANI solution on the quartz substrate before being dried in air and repeated for 6 times.

3. Results and Discussion

3.1 XRD Analysis of LDH Precursor

The XRD patterns of the ZnAl-CO_3^{2-}-LDH precursor are shown in Fig. 1a. Apparently, the XRD patterns for ZnAl-LDH exhibit the characteristic reflections of LDH materials with *00l* peaks, which represent the layered structure [23]. No obvious peaks of impurities were discerned, indicating the high purity of the product. In addition, the sharp and symmetric features of the diffraction peaks strongly suggest that the produced ZnAl-CO_3^{2-}-LDH is highly crystallized with a three-dimensional order. After being ion exchanged with NO_3^-, the *00l* peaks of ZnAl-LDH are moved to small angle (Fig. 1b), which means the gallery height increases after ion exchange. By calculating with Bragg function, the gallery height is increased from 0.75 nm of ZnAl-CO_3^{2-}-LDH to 0.89 nm of NO_3^- intercalated ZnAl-LDH, suggesting the successful exchange of the guest anion form CO_3^{2-} to NO_3^- [30]. After being delaminated into colloid suspension, all the characteristic reflections of LDH are replaced by an obvious bump peak in the range of 20-30° (Fig. 3b) which is due to the scattering of nanosheets gel [30].

3.2 UV-vis Absorption Spectroscopy of (ZnAl-LDH/PANI)$_n$ Multilayer Films

Multilayer films were obtained by alternately dipping a quartz glass slide into a colloidal suspension of the LDH nanosheets and PANI solution. The multilayer

build-up process of the film was monitored by UV-Vis spectroscopy after each deposition cycle. Fig. 2a shows the UV-vis absorption spectra of $(ZnAl\text{-}LDH/PANI)_n$ multilayer films with various bilayers numbers (n) deposited on quartz substrates and the pure PANI film on quartz substrate. The UV-vis spectrum of pure PANI film is shown in the dotted line from Fig. 2a, which indicates that there are two adsorption bands belongs to PANI near 300 nm (- * transition of benzoid ring) [32] and 550 nm (benzoid-quinoid structure) [33], respectively. After the PANI is assembled and intercalated between the LDH nanosheets, there are slight red shifts of absorption bands for PANI in the $(ZnAl\text{-}LDH/PANI)_n$ multilayer films, which can be attributed to the electrostatic interaction between ZnAl-LDH nanosheets and PANI. Furthermore, it is observed that the absorption bands at about 324 and 600 nm are linearly correlated with the number of bilayers (Fig. 2b). It can be seen that the absorption intensity increases linearly with the increase of the deposition cycles, which indicates a stepwise and regular film growth in thickness.

3.3 Morphology and Structural Characterization of $(ZnAl\text{-}LDH/PANI)_n$ Multilayer Films

A typical top views of the SEM images for $(ZnAl\text{-}LDH/PANI)_n$ multilayer films (Fig. 3) confirm that the surfaces of the films are microscopy smooth and uniform. Fig. 4 shows the AFM topographical images which give the morphology and roughness information of the multilayer films. The value of root-mean-square (rms) roughness of the multilayer films increases slowly from 3.213 nm for 12 bilayers (n = 12) to 5.118 nm for 30 bilayers (n = 30), indicating that all the multilayer films have relatively

smooth surfaces. The deposited process of $(ZnAl\text{-}LDH/PANI)_n$ multilayer films was further monitored by SEM and AFM. The side-views of SEM (Fig. 5) illustrate the dependence of the thickness of the ZnAl-LDH/PANI multilayer films on the bilayers number n. The approximately linear that increase from 24 nm for 12 bilayers to 59 nm for 30 bilayers, suggests the average thickness of one ZnAl-LDH/PANI unit is about 2.0 nm.

3.4 Gas Sensing Characterization for $(ZnAl\text{-}LDH/PANI)_n$ Multilayer Films (n = 12, 30)

In this paper, the ammonia-sensing behavior of multilayer films was observed by measuring the resistance change when the multilayer films were exposed to ammonia. Fig. 6 shows the response and recovery curves of $(ZnAl\text{-}LDH/PANI)_{12}$ multilayer film and $(ZnAl\text{-}LDH/PANI)_{30}$ multilayer film. It can be seen that all the $(ZnAl\text{-}LDH/PANI)_n$ multilayer films have a reversible response to NH_3 at room temperature. In Fig. 6, for the first 90 s the multilayer films were exposed to air, after that the air was replaced by 1000 ppm ammonia in air and remained as such for 450 s before the environment was switched back to air. It is found that the response values to 1000 ppm ammonia increase from 14 to 16 as the bilayers numbers increase from 12 to 30. In addition, response and recovery speeds are vital parameters to evaluate the sensing performance, especially for sensing materials which response at low working temperature as room temperature. The response and recovery time of $(ZnAl\text{-}LDH/PANI)_{12}$ at room temperature are calculated to be 120 and 150 s, respectively. For $(ZnAl\text{-}LDH/PANI)_{30}$, though the response increases from 14 of $(ZnAl\text{-}LDH/PANI)_{12}$ multilayer film to 16, the response/recovery

are prolonged to 150/240 s.

At a constant temperature, the response of gas sensors would change with the concentrations of ammonia. Fig. 7 shows the correlation between the concentrations and the responses of $(ZnAl\text{-}LDH/PANI)_n$ multilayer films (n = 12 and 30) at room temperature (25°C). It's obvious that the $(ZnAl\text{-}LDH/PANI)_{30}$ multilayer film has a higher response than $(ZnAl\text{-}LDH/PANI)_{12}$ multilayer film as it has more bilayers. Besides, these multilayer films can detect ammonia gas down to 100 ppm, and the corresponding values are 1.8 for $(ZnAl\text{-}LDH/PANI)_{12}$ multilayer film and 2.4 for $(ZnAl\text{-}LDH/PANI)_{30}$ multilayer film, respectively. With an increase in gas concentration, the responses increase remarkably. The responses are 3.6, 8, 14, 22, 34 and 38 for $(ZnAl\text{-}LDH/PANI)_{12}$ multilayer film to 200, 500, 1000, 2000, 5000 and 10000 ppm ammonia, and the corresponding values for $(ZnAl\text{-}LDH/PANI)_{30}$ multilayer film are 4.6, 9, 16, 24, 38 and 44, respectively.

For comparison, the pure PANI film and ZnAl-LDH film were prepared by solvent evaporation at 100°C under vacuum for 48 h. The gas sensing behavior of the two films were observed under the same conditions as $(ZnAl\text{-}LDH/PANI)_n$ multilayer films. As shown in Fig. 8, the pure PANI film shows a very low response to 1000 ppm ammonia (1.18) as well as very long response and recovery time (more than 300 s and 400 s, respectively), whereas the pure ZnAl-LDH film has almost no response to ammonia. Moreover, the ammonia sensing performance of $(ZnAl\text{-}LDH/PANI)_n$ multilayer films to ammonia is also comparable with the previous studies of PANI or PANI-based gas sensing materials [3, 4, 16, 34-37], as the multilayer films have a relatively high response, short response/recovery time and good recoverability.

Similar to the previous reports about polyaniline-based gas sensors [7, 34, 38], the

ammonia sensing mechanism of polyaniline can be explained as follows, that is, the resistance change will be modulated by the protonation-deprotonation of polyaniline brought by ammonia. When ammonia is adsorbed onto or into the polymer, ammonia molecules would grab protons from N^+-H sites of PANI to form NH_4^+. This deprotonation process of PANI will reduce polyaniline from the emeraldine salt state to the emeraldine base state, leading to an increase of electrical resistance. When the sensor is in ambient air circumstance, the process is reversed: NH_4^+ will be decomposed to form ammonia gas and a proton which will be given back to PANI, therefore, the initial doping level and electrical resistance of polyaniline will be recovered [15, 38]. In this paper, it is worth mentioning that the LDH nanosheets play a critical effect on the enhancement of the gas sensing properties of PANI. As ZnAl-LDH nanosheets provide a rigid, confined and stable microenvironment for the PANI with a relatively uniform orientation and a suppressed aggregation, which may increase the void for reaction with ammonia molecule, and then the ammonia sensing response has been largely enhanced.

Furthermore, the selectivity of gas sensor is also an important factor for further application. To illustrate the gas selectivity of $(ZnAl\text{-}LDH/PANI)_{12}$ multilayer film and $(ZnAl\text{-}LDH/PANI)_{30}$ multilayer film, the responses of the multilayer films to different gases as NO_2, CO, H_2, CH_4, C_2H_2 and C_2H_5OH with 10000 ppm, which is ten times concentration of ammonia, was conducted and their responses were compared with the response of the sensor towards 1000 ppm of ammonia in Fig. 9. It is found that both of them exhibit very high response to ammonia but low responses to NO_2, CO, H_2, and almost no significant response to CH_4, C_2H_2 and C_2H_5OH even with ten times

concentration of ammonia, indicating that this kind of $(ZnAl\text{-}LDH/PANI)_n$ multilayer films are good candidates for future use to detect ammonia.

4. Conclusions

The ordered inorganic-organic multilayer films of LDH/PANI with ultrathin thickness were fabricated by the LBL deposition technique in this work which exhibit application as a gas sensor for ammonia. The UV-vis absorption shows stepwise and regular film growth procedure. The SEM and AFM images further confirm the films possess the organized morphology and structure with 2 nm's thickness per bilayer. In comparison with the pure PANI film and ZnAl-LDH film, the obtained $(ZnAl\text{-}LDH/PANI)_{12}$ multilayer film and $(ZnAl\text{-}LDH/PANI)_{30}$ multilayer film show high response, short response/recovery time, good reversibility as well as high selectivity to ammonia at room temperature. The rigid LDH nanosheets isolate PANI molecules from each other ad eliminate the aggregation and interaction between molecules. Therefore, this work provides a facile and feasible methodology for the fabrication of novel gas sensor. By virtue of the highly tunable compositions both for inorganic and organic parts, these multilayer films can be potentially applied in gas sensing field.

Acknowledgments:

This work was supported by the National Natural Science Foundation of China (21001014), Beijing Natural Science Foundation (2113049), Program for Changjiang Scholars and Innovative Research Team in University (IRT1205).

References

[1] B. Timmer, W. Olthuis, A.v.d. Berg, Ammonia sensors and their applications-a review, Sens. Actuators B: Chem., 107 (2005) 666-677.

[2] A.A. Khan, U. Baig, M. Khalid, Ammonia vapor sensing properties of polyaniline-titanium (IV) phosphate cation exchange nanocomposite, J. Hazard. Mater., 186 (2011) 2037-2042.

[3] D. Verma, V. Dutta, Role of novel microstructure of polyaniline-CSA thin film in ammonia sensing at room temperature, Sens. Actuators B: Chem., 134 (2008) 373-376.

[4] G.D. Khuspe, D.K. Bandgar, S. Sen, V.B. Patil, Fussy nanofibrous network of polyaniline (PANI) for NH_3 detection, Synth. Met., 162 (2012) 1822-1827.

[5] M.M. Galera, E. Cho, E. Tuuguu, S.-J. Park, C. Lee, W.-J. Chung, Effects of pollutant concentration ratio on the simultaneous removal of NH_3, H_2S and toluene gases using rock wool-compost biofilter. J. Hazard. Mater., 152 (2008) 624-631.

[6] R.E. de la Hoz, D.P. Schlueter, W.N. Rom, Chronic lung disease secondary to ammonia inhalation injury: a report on three cases, Am. J. Ind. Med., 29 (1996) 209-214.

[7] D. Nicolas-Debarnot, F. Poncin-Epaillard, Polyaniline as a new sensitive layer for gas sensors, Anal. Chim. Acta, 475 (2003) 1-15.

[8] M. Matsuguchi, J. Io, G. Sugiyama, Y. Sakai, Effect of NH_3 gas on the electrical conductivity of polyaniline blend films, Synth. Met., 128 (2002) 15-19.

[9] H. Tai, Y. Jiang, G. Xie, J. Yu, X. Chen, Z. Ying, Influence of polymerization temperature on NH_3 response of PANI/TiO_2 thin film gas sensor, Sens. Actuators B: Chem., 129 (2008) 319-326.

[10] X.B. Yan, Z.J. Han, Y. Yang, B.K. Tay, NO_2 gas sensing with polyaniline nanofibers synthesized by a facile aqueous/organic interfacial polymerization, Sens. Actuators B: Chem., 123 (2007) 107-113.

[11] M.K. Ram, Ö. Yavuz, V. Lahsangah, M. Aldissi, CO gas sensing from ultrathin nano-composite conducting polymer film, Sens. Actuators B: Chem., 106 (2005) 750-757.

[12] M.M. Ayad, G. El-Hefnawey, N.L. Torad, A sensor of alcohol vapours based on thin polyaniline base film and quartz crystal microbalance. J. Hazard. Mater., 168 (2009) 85-88.

[13] Q. Lin, Y. Li, M. Yang, Gas sensing properties of layer-by-layer self-assembled ultrathin film of polyaniline/titanium dioxide, Synth. Met., 162 (2012) 2242-2249.

[14] L. Geng, Y. Zhao, X. Huang, S. Wang, S. Zhang, S. Wu, Characterization and gas sensitivity study of polyaniline/SnO_2 hybrid material prepared by hydrothermal route, Sens. Actuators B: Chem., 120 (2007) 568-572.

[15] T. Zhang, M.B. Nix, B.Y. Yoo, M.A. Deshusses, N.V. Myung, Electrochemically Functionalized Single-Walled Carbon Nanotube Gas Sensor, Electroanalysis, 18 (2006) 1153-1158.

[16] N.G. Deshpande, Y.G. Gudage, R. Sharma, J.C. Vyas, J.B. Kim, Y.P. Lee, Studies on tin oxide-intercalated polyaniline nanocomposite for ammonia gas sensing applications, Sens. Actuators B: Chem., 138 (2009) 76-84.

[17] X. Sui, Y. Chu, S. Xing, C. Liu, Synthesis of PANI/AgCl, PANI/$BaSO_4$ and PANI/TiO_2 nanocomposites in CTAB/hexanol/water reverse micelle, Mater. Lett., 58

(2004) 1255-1259.

[18] G.W. Ho, Gas Sensor with Nanostructured Oxide Semiconductor Materials. Sci. Adv. Mater. 3 (2011) 150–168.

[19] N. Du, H. Zhang, B.D. Chen, X. Y. Ma, Z. H. Liu, J. B. Wu, D. R. Yang, Porous Indium Oxide Nanotubes: Layer-by-Layer Assembly on Carbon-Nanotube Templates and Application for Room-Temperature NH_3 Gas Sensors. Adv. Mater. 19 (2007) 1641–1645.

[20] J.H. Kim, S.H. Kim, S. Shiratori, Fabrication of Nanoporous and Hetero Structure Thin Film via a Layer-by-Layer Self Assembly Method for A Gas Sensor. Sens. Actuator B: Chem., 102 (2004) 241–247.

[21]P.G. Su, C.C. Shiu, Flexible H_2 Sensor Fabricated by Layer-by-Layer Self-Assembly of Thin Films of Polypyrrole and Modified in Situ with Pt Nanoparticles. Sens. Actuator B: Chem., 157 (2011), 275–281.

[22] D. Yan, J. Lu, J. Ma, M. Wei, X. Wang, D.G Evans, X. Duan, Anionic Poly(p-Phenylenevinylene)/Layered Double Hydroxide Ordered Ultrathin Films with Multiple Quantum Well Structure: A Combined Experimental and Theoretical Study, Langmuir, 26 (2010) 7007-7014.

[23] E. Dvininov, M. Ignat, P. Barvinschi, M. A. Smithers, E. Popovici, New SnO_2/MgAl-layered double hydroxide composites as photocatalysts for cationic dyes bleaching. J. Hazard. Mater., 177 (2010) 150-158.

[24] Y. Guo, Y. Xiao, L. Zhang, Y. Song, Fabrication of $(Calcein–ZnS)_n$ Ordered

Ultrathin Films on the Basis of Layered Double Hydroxide and Its Ethanol Sensing Behavior, Ind. Eng. Chem. Res., 51 (2012) 8966-8973.

[25] J. Han, D. Yan, W. Shi, J. Ma, H. Yan, M. Wei, D.G Evans, X. Duan, Layer-by-Layer Ultrathin Films of Azobenzene-Containing Polymer/Layered Double Hydroxides with Reversible Photoresponsive Behavior, J. Phys. Chem. B, 114 (2010) 5678-5685.

[26] X. Wang, J. Lu, W. Shi, F. Li, M. Wei, D.G Evans, X. Duan, A Thermochromic Thin Film Based on Host-Guest Interactions in a Layered Double Hydroxide, Langmuir, 26 (2010) 1247-1253.

[27] M. Shao, M. Wei, D.G Evans, X. Duan, Magnetic-field-assisted assembly of CoFe layered double hydroxide ultrathin films with enhanced electrochemical behavior and magnetic anisotropy, Chem. Commun., 47 (2011) 3171.

[28] A. Domenech, E. Coronado, N. Lardies, C. M. Gastaldo, M. T. Domenech-Carbo, A. Ribera, Solid-state electrochemistry of LDH-supported polyaniline hybrid inorganic-organic material, J. Electroanal. Chem., 624 (2008) 275-286.

[29] S. Huang, X. Cen, H. Peng, S. Guo, W. Wang, T. Liu, Heterogeneous ultrathin films of poly (vinyl alcohol)/layered double hydroxide and montmorillonite nanosheets via layer-by-layer assembly, J. Phys. Chem. B, 113 (2009) 15225-15230.

[30] Z. Liu, R. Ma, M. Osada, N. Iyi, Y. Ebina, K. Takada, T. Sasaki, Synthesis, Anion Exchange, and Delamination of Co-Al Layered Double Hydroxide: Assembly of the Exfoliated Nanosheet/Polyanion Composite Films and Magneto-Optical Studies, J. Am. Chem. Soc., 128 (2006) 4872-4880.

[31] N. Iyi, Y. Ebina, T. Sasaki, Synthesis and characterization of water-swellable LDH (layered double hydroxide) hybrids containing sulfonate-type intercalant, J. Mater. Chem., 21 (2011) 8085.

[32] J.E. Albuquerque, L.H.C. Mattoso, D.T. Balogh, R.M. Faria, J.G. Masters, A.G. MacDiarmid, A simple method to estimate the oxidation state of polyanilines, Synth. Met., 113 (2000) 19-22.

[33] H. Xie, Y. Ma, J. Guo, Secondary doping phenomena of two conductive polyaniline composites, Synth. Met., 123 (2001) 47-52.

[34] V.V Chabukswar, S. Pethkar, A.A Athawale, Acrylic acid doped polyaniline as an ammonia sensor, Sens. Actuators B: Chem., 77 (2001) 657-663.

[35] C.V. Tuan, M.A. Tuan, N.V. Hieu, T. Trung, Electrochemical synthesis of polyaniline nanowires on Pt interdigitated microelectrode for room temperature NH_3 gas sensor application, Curr. Appl. Phys., 12 (2012) 1011-1016.

[36] M. Matsuguchi, T. Asahi, Properties and stability of polyaniline nanofiber ammonia sensors fabricated by novel on-substrate method, Sens. Actuators B: Chem., 160 (2011) 999-1004.

[37] J. Yun, J.S. Im, H.I. Kim, Y.S. Lee, Effect of oxyfluorination on gas sensing behavior of polyaniline-coated multi-walled carbon nanotubes, Appl. Surf. Sci., 258 (2012) 3462-3468.

[38] H. Tai, Y. Jiang, G. Xie, J. Yu, X. Chen, Fabrication and gas sensitivity of polyaniline–titanium dioxide nanocomposite thin film, Sens. Actuators B: Chem., 125 (2007) 644-650.

Captions of Schemes and Figures

Scheme 1 LBL assembly process for $(ZnAl\text{-}LDH/PANI)_n$ films.

Fig. 1 XRD patterns of a. ZnAl-CO_3^{2-}-LDH, b. ZnAl-NO_3^--LDH, c. ZnAl-LDH nanosheets.

Fig. 2 a. UV-vis absorption spectra of the $(ZnAl\text{-}LDH/PANI)_n$ multilayer films with bilayer numbers of n ((n = 3, 6, 9, 12, 18, 24, 30 and the dotted line belongs to PANI film), b. Linear relationship of the absorbances at 324 and 600 nm with bilayer numbers of n (n = 3, 6, 9, 12, 18, 24, 30) .

Fig. 3 Top-views of SEM for $(ZnAl\text{-}LDH/PANI)_n$ multilayer films with n = 6, 12, 18, 24, 30, respectively.

Fig. 4 AFM for $(ZnAl\text{-}LDH/PANI)_n$ multilayer films with n = 6, 12, 18, 24, 30, respectively.

Fig. 5 Thicknesses of $(ZnAl\text{-}LDH/PANI)_n$ multilayer films as a function of n; the insets show the side-view SEM images with n = 6, 12, 18, 24, 30.

Fig. 6 Response and recovery curves of $(ZnAl\text{-}LDH/PANI)_n$ multilayer films to 1000 ppm ammonia at room temperature (a. n = 12, b. n = 30).

Fig. 7 Responses of $(ZnAl\text{-}LDH/PANI)_n$ multilayer film to different concentration of ammonia at room temperature (a. n = 12, b. n = 30).

Fig. 8 Response and recovery curve of pure PANI film to 1000 ppm ammonia at room temperature.

Fig. 9 Gas responses of $(ZnAl\text{-}LDH/PANI)_n$ multilayer films to 1000 ppm of ammonia and 10000 ppm of NO_2, H_2, CO, CH_4, C_2H_2 and ethanol at room temperature.

Highlights:

$(ZnAl\text{-}LDH/PANI)_n$ multilayer films have been fabricated via a layer-by-layer assembly way.

The multilayer films have relatively ordered morphology and controllable thickness.

The multilayer films show extremely high selectivity to ammonia at room temperature.

Graphical Abstract

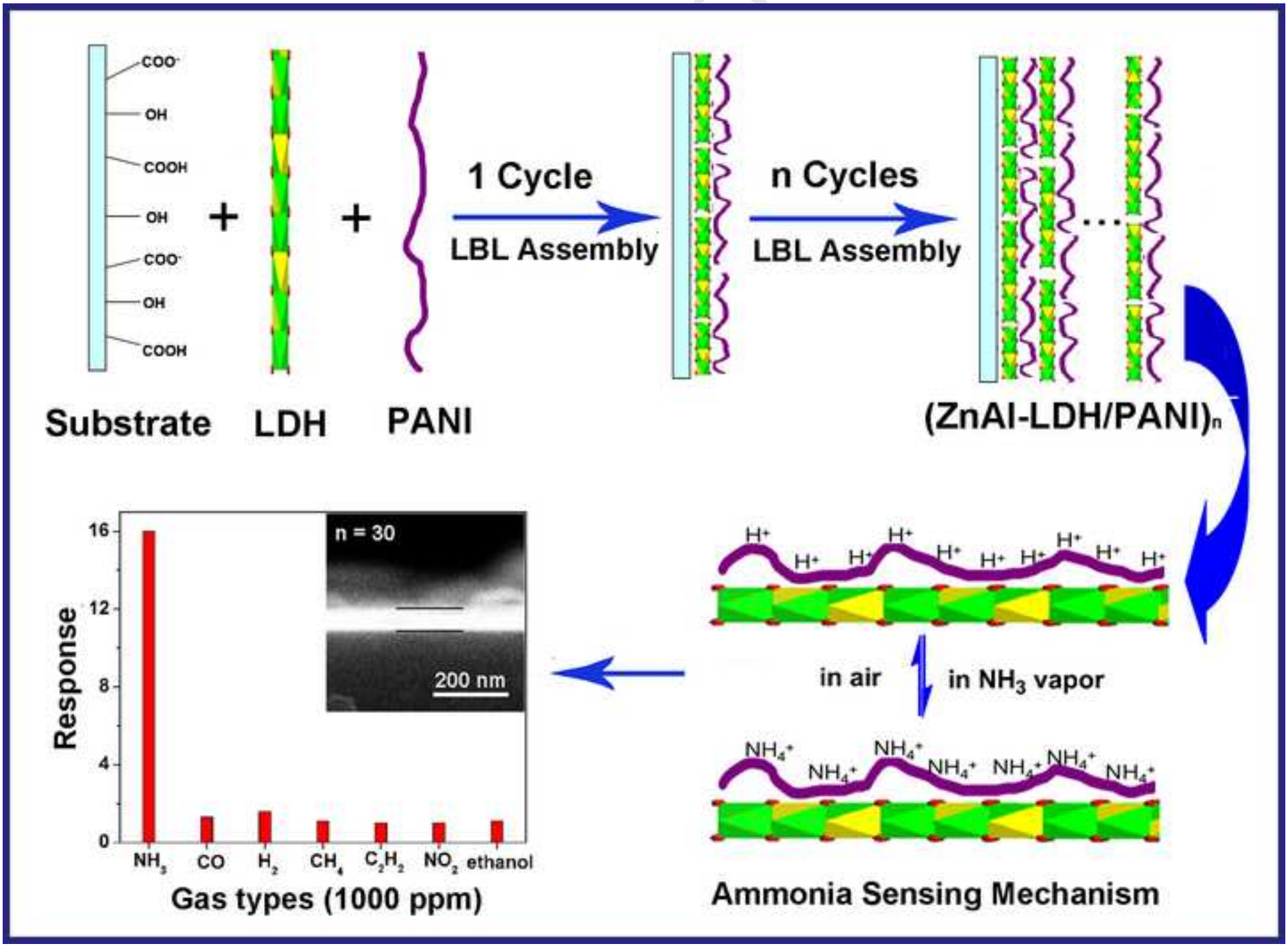

Scheme 1

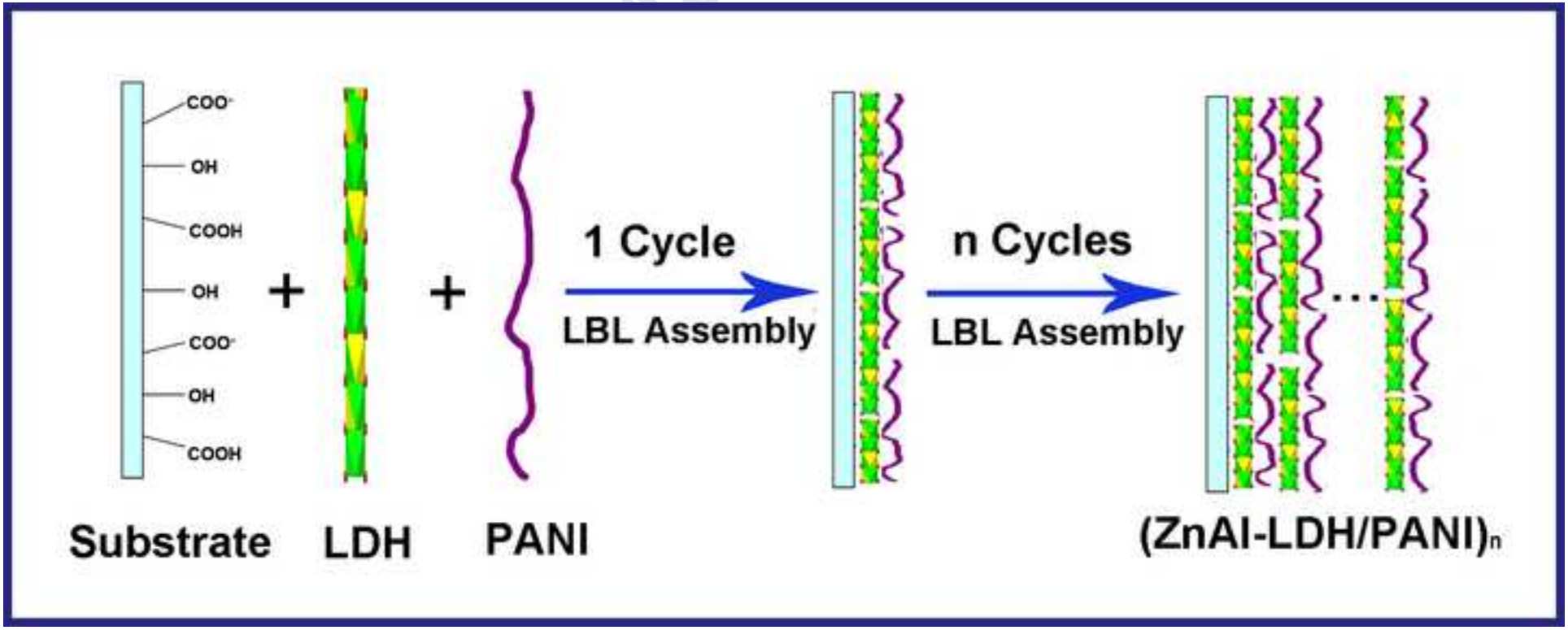
COO⁻
OH
COOH
OH
COO⁻
OH
COOH
+
+
1 Cycle
LBL Assembly
n Cycles
LBL Assembly
Substrate
LDH
PANI
(ZnAl-LDH/PANI)n

Figure 1

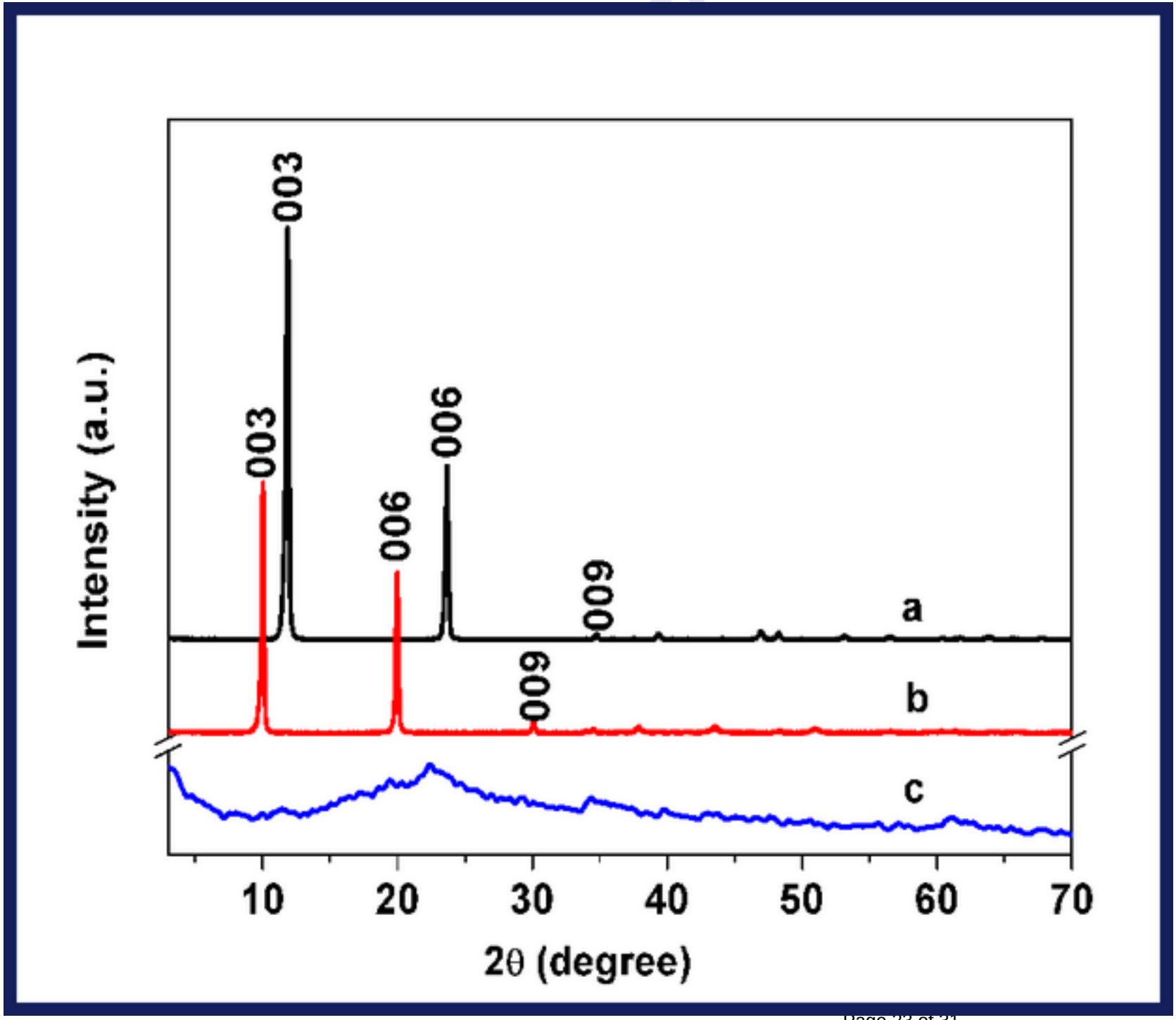
Intensity (a.u.)
003
003
006
006
009
009
a
b
c
10
20
30
40
50
60
70
2θ (degree)

Figure 2

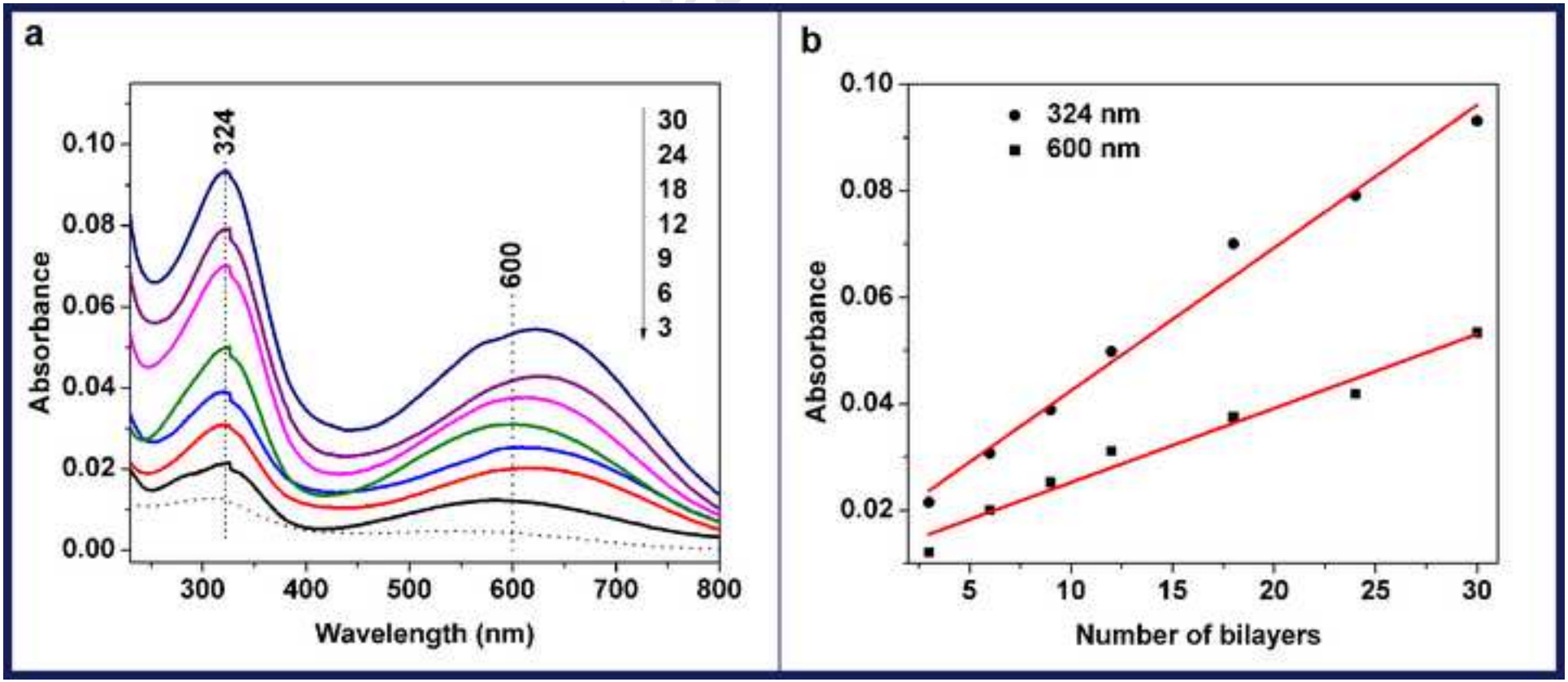
a
Absorbance
Wavelength (nm)
324
600
30
24
18
12
9
6
3
0.00
0.02
0.04
0.06
0.08
0.10
300
400
500
600
700
800
b
Absorbance
Number of bilayers
324 nm
600 nm
0.02
0.04
0.06
0.08
0.10
5
10
15
20
25
30

Figure 3

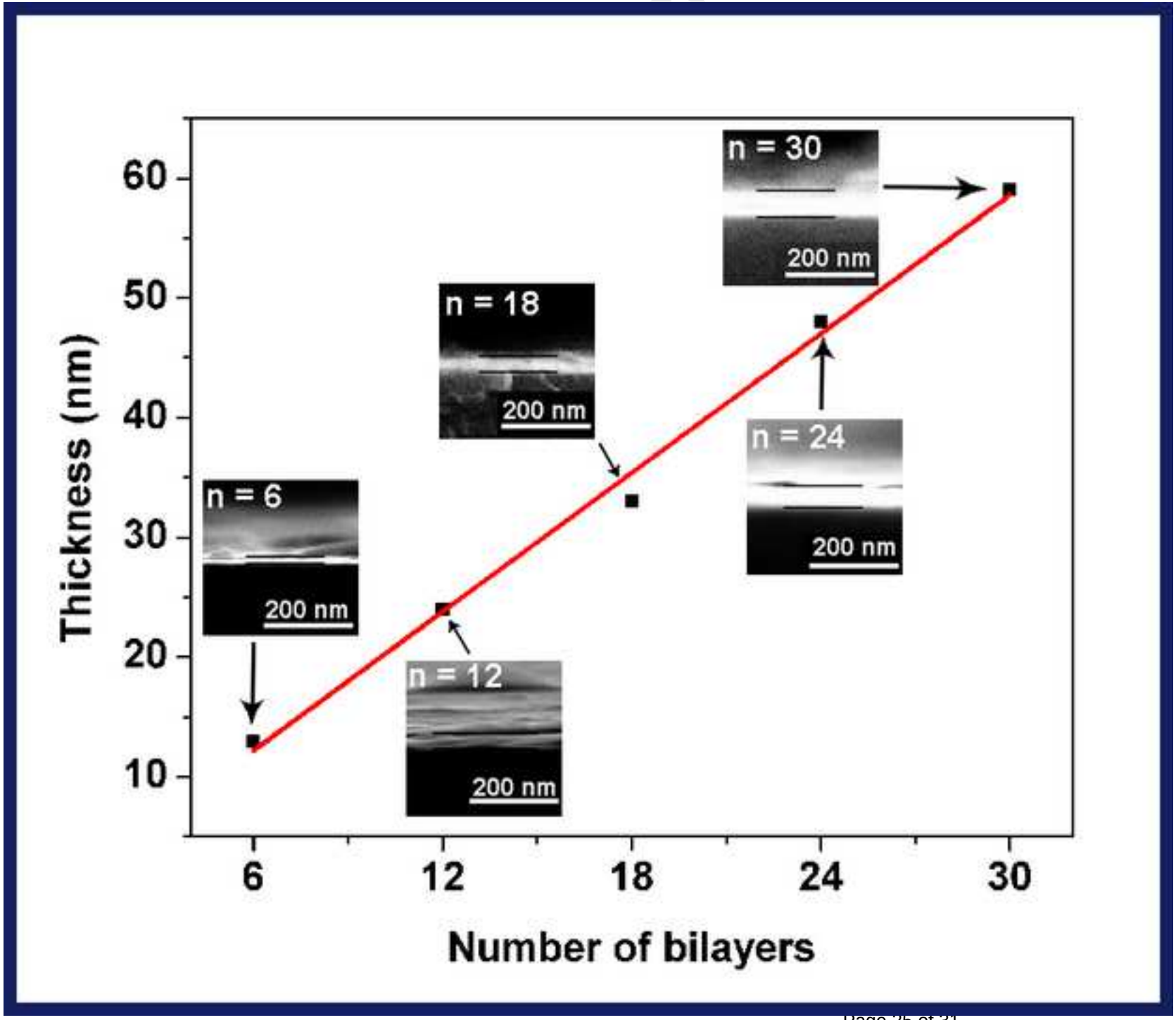
Thickness (nm)
60
50
40
30
20
10
6
12
18
24
30
Number of bilayers
n = 6
200 nm
n = 12
200 nm
n = 18
200 nm
n = 24
200 nm
n = 30
200 nm

Figure 4

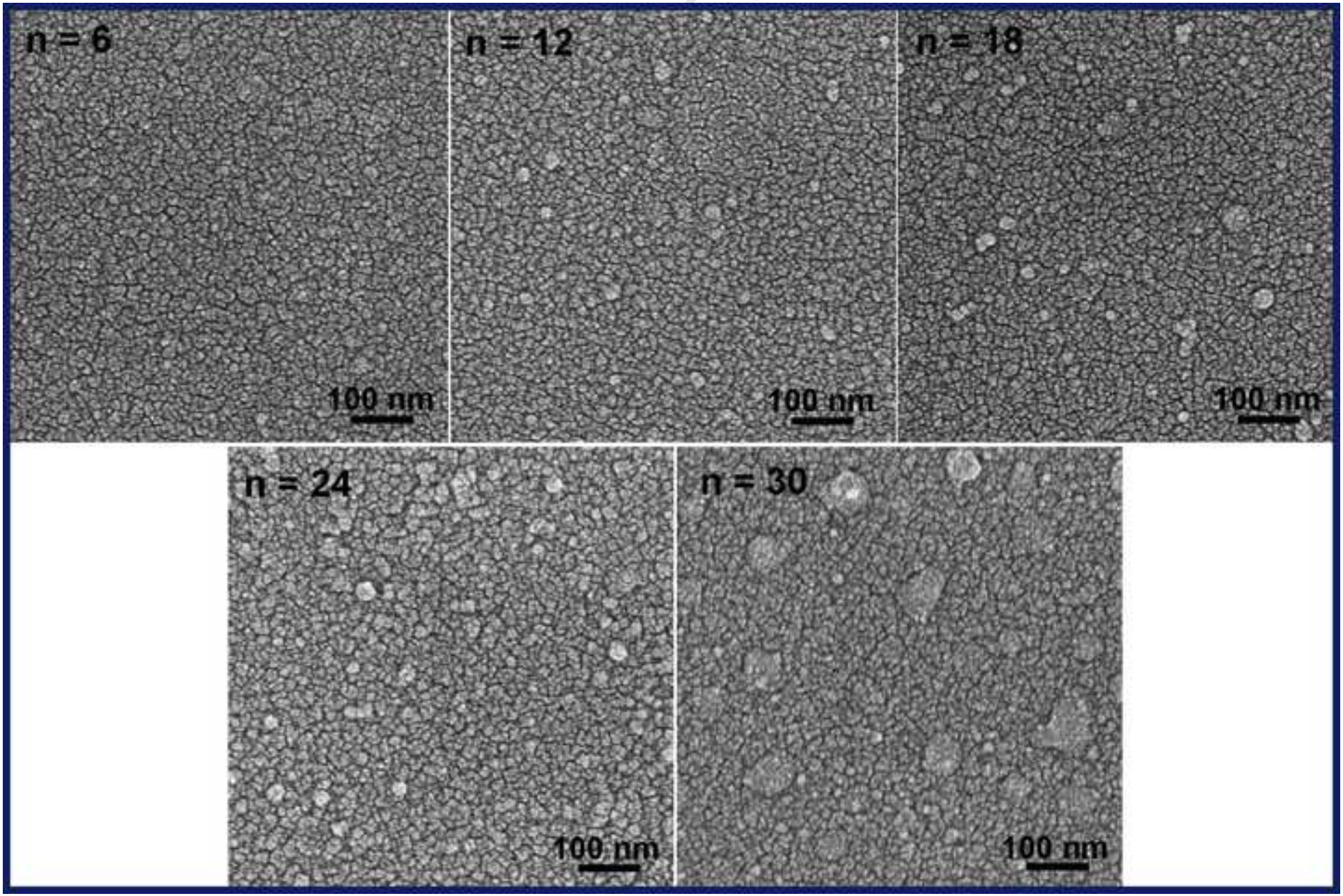

Figure 5

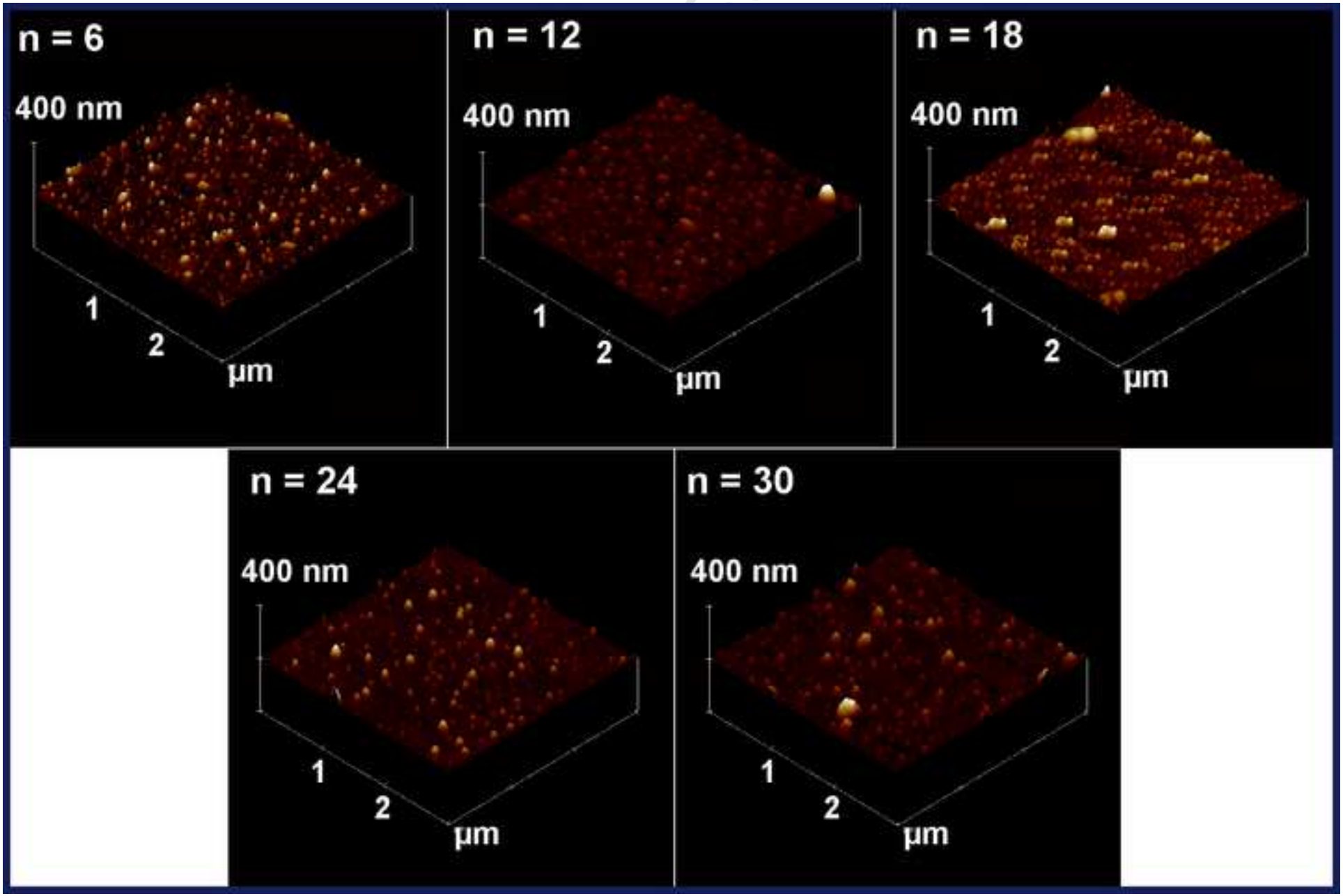
n = 6
400 nm
1
2
µm
n = 12
400 nm
1
2
µm
n = 18
400 nm
1
2
µm
n = 24
400 nm
1
2
µm
n = 30
400 nm
1
2
µm

Figure 6

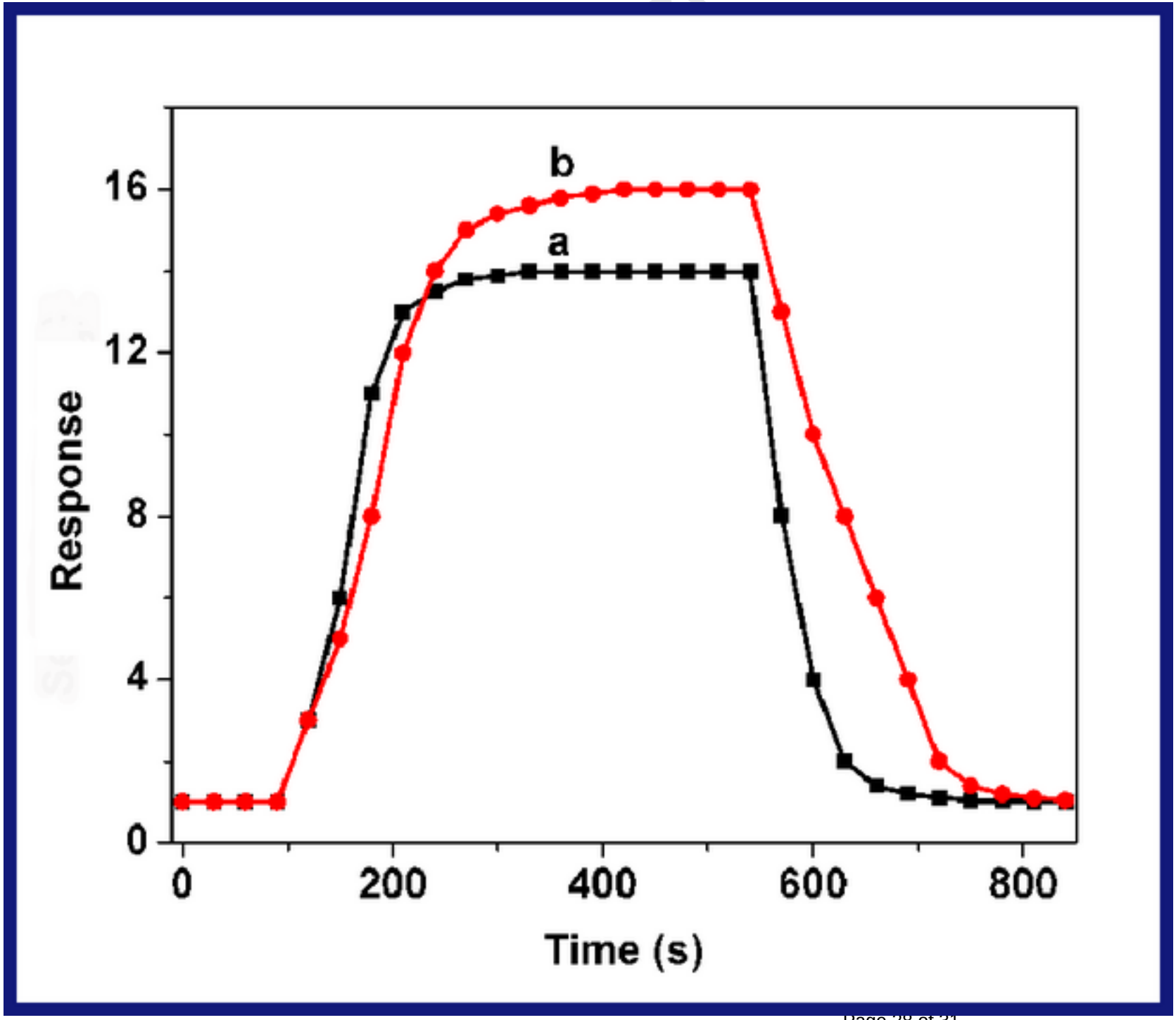

Figure 7

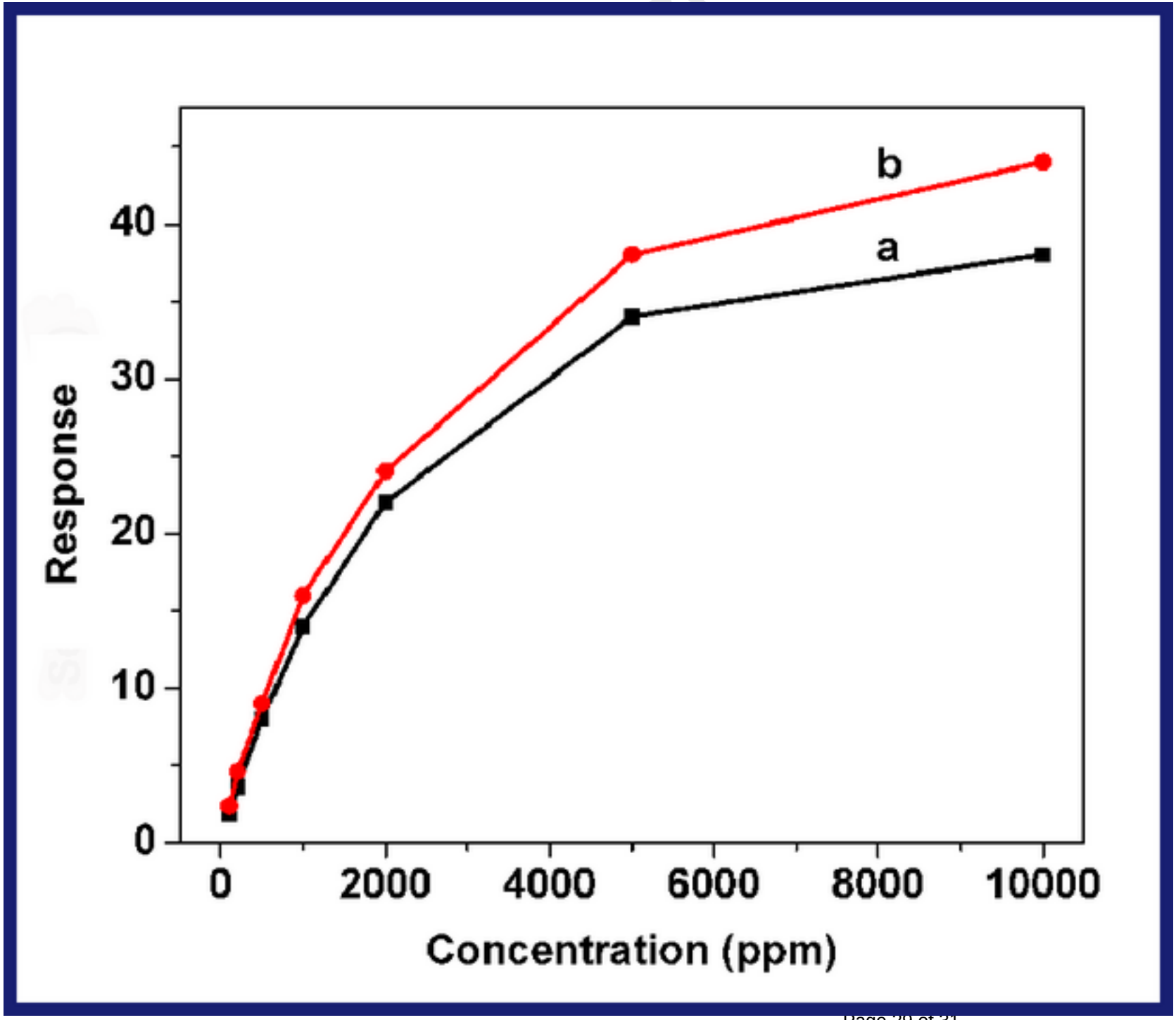
b
a
Response
0
10
20
30
40
0
2000
4000
6000
8000
10000
Concentration (ppm)

Figure 8

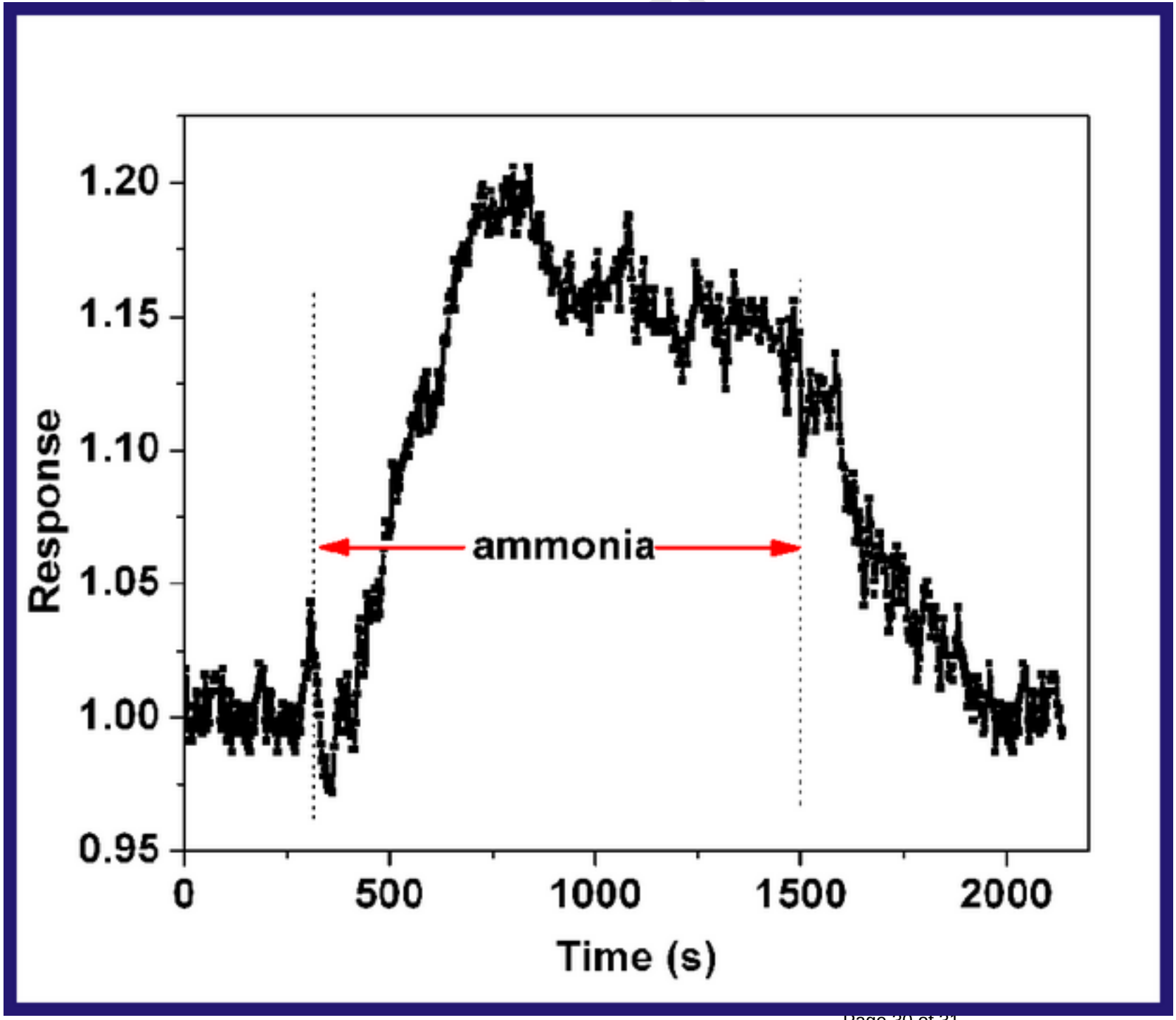
1.20
1.15
1.10
1.05
1.00
0.95
Response
ammonia
0
500
1000
1500
2000
Time (s)

Figure 9

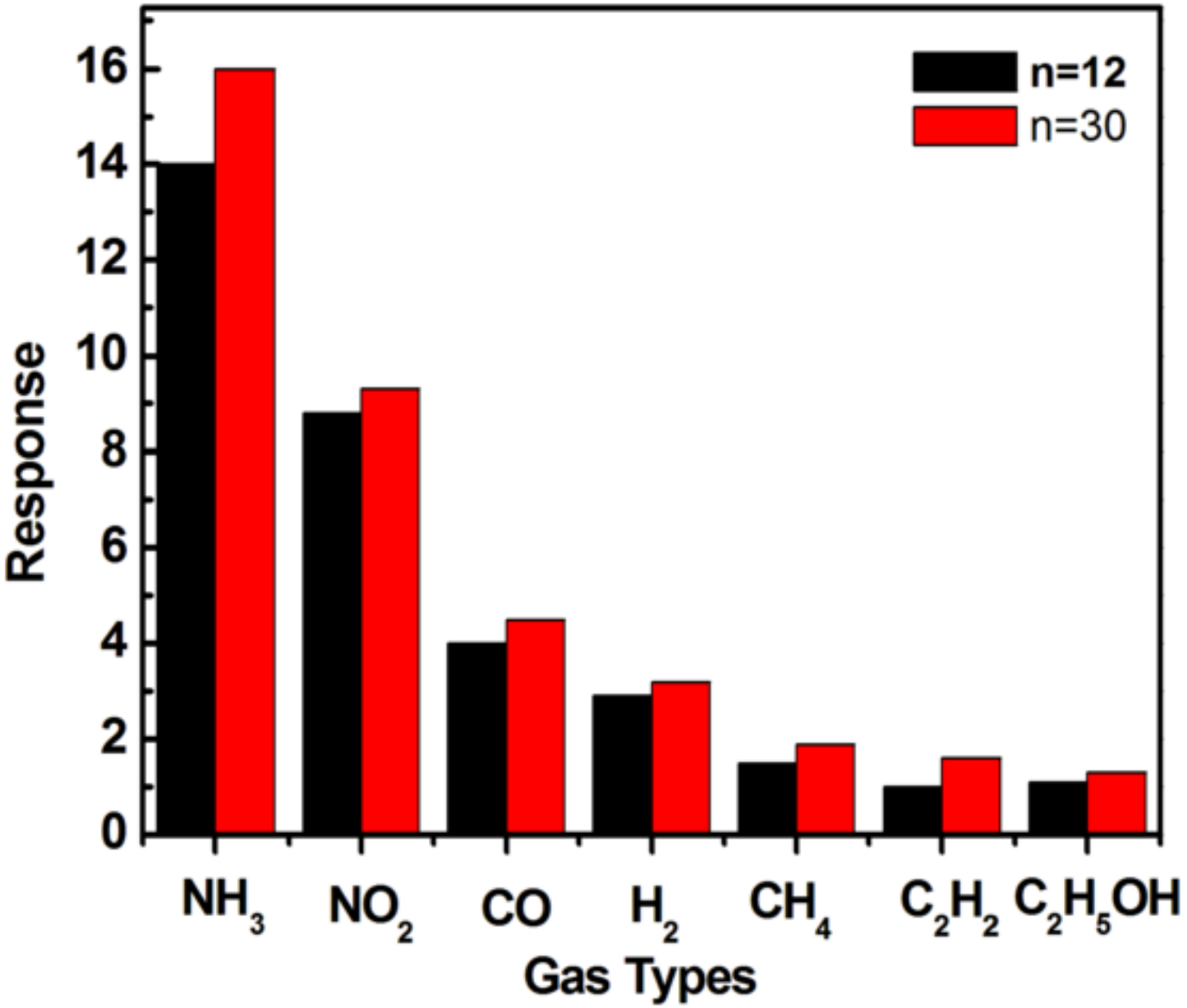
n=12
n=30
Response
0
2
4
6
8
10
12
14
16
NH3
NO2
CO
H2
CH4
C2H2
C2H5OH
Gas Types